Acta Ophthalmologica

Safety of femtosecond laser-assisted cataract surgery: assessment of aqueous humour and lens capsule

A-Yong Yu, Cai-Xia Lin, Qin-Mei Wang, Mei-Qing Zheng and Xiao-Yi Qin

The Eye Hospital of Wenzhou Medical University, Wenzhou, Zhejiang, China

ABSTRACT.

Purpose: **To investigate the effect of femtosecond laser-assisted cataract surgery (FLACS) on aqueous humour and lens capsule.**

Methods: **This prospective randomized comparative study enrolled 19 eyes that underwent FLACS as the trial group and 20 eyes that underwent conventional phacoemulsification as the control group. The femtosecond laser platform (LLS-fs 3D; LensAR, Orlando, FL, USA) was used to generate capsulotomy (laser energy 8 μJ) and lens fragmentation (laser energy 10 μJ). Morphology of the cutting edge and cells of anterior capsule was assessed by light microscopy. The proteins in the aqueous humour were identified by mass spectrometry (Ultraflex III TOF/TOF; Bruker Dalton, Bremen, Germany). Electrolyte in the aqueous humour was detected by a chemistry analyzer (Aeroset Clinical Chemistry Analyzer; Abbott Laboratories, Abbott Park, IL, USA).**

Results: **The cutting edge of anterior capsule was saw-tooth-shaped under magnification of 200× and 400× in the trial group, while it was smooth in the control group. Intact cells were found in the boundary area next to the cutting edge of anterior capsule in both groups. β-Crystallin B1, γ-crystallin S and transferrin were detected in the aqueous humour in the trial group. The concentrations of K^+, Na^+ and Cl^- in the aqueous humour in the trial group differed significantly from those in the control group ($p = 0.02$, 0.03 and 0.04, respectively).**

Conclusion: **Femtosecond laser-assisted cataract surgery (FLACS) causes release of transferrin and crystallin from lens to aqueous humour and results in significant changes in the concentrations of K^+, Na^+ and Cl^- in aqueous humour. However, these changes due to FLACS have no clinical significance or toxicity.**

Key words: aqueous humour – cataract – femtosecond laser – lens capsule

Acta Ophthalmol.

doi: 10.1111/aos.13022

Introduction

Since femtosecond laser was approved for cataract surgery by the FDA in 2010 (He et al. 2011), femtosecond laser-assisted cataract surgery (FLACS) has demonstrated high precision of capsulotomy, reduced phacoemulsification power and time, and comparable refractive outcome in clinic (Nagy et al. 2009; Palanker et al. 2010; Alio 2011; Friedman et al. 2011; Krarup et al. 2014; Yu et al. 2015). Femtosecond laser-assisted cataract surgery (FLACS) produces enormous energy on a very narrow space and dissects tissue by photodisruption (Hansen et al. 2013). It was reported that prostaglandins rise immediately after femtosecond laser treatment (Schultz et al. 2013), and cavitation bubbles derived from the photodisruption process lead to an acidic shift of the aqueous humour pH as a result of the transformation of carbon dioxide to carbonic acid (Rossi et al. 2015), which might be prone to the intraoperative laser-induced miosis. However, it is still unknown whether there are toxic substances produced due to photochemical or high-energy physical effects of femtosecond laser during FLACS. If yes, whether the waiting interval from completion of femtosecond laser operation to the beginning of phacoemulsification is questionable due to the possibility of dispersion of such substances? This study aimed to investigate the effect of FLACS on aqueous humour and lens capsule.

Patients and Methods

This prospective randomized comparative study enrolled consecutive patients having cataract surgery at the Eye Hospital of Wenzhou Medical University from 21 October to 20 November 2013. All patients underwent a comprehensive ophthalmologic examination including slit-lamp microscopy, corneal topography and dilated funduscopy. The inclusion criteria included normal cornea, and dilated pupillary diameter greater than 6 mm. Exclusion criteria were previous ocular trauma or surgery, and any local or

systemic abnormalities other than cataract, such as extensive corneal scarring, pseudoexfoliation syndrome, glaucoma, ocular inflammation, retinal abnormalities, infections and diabetes mellitus.

The surgical option of FLACS (trial group) or traditional phacoemulsification (control group) was randomly assigned after each patient was fully informed about the details and possible risks inherent to this study. All patients were followed up 6 months after surgery. This study was approved by the Ethics Committee at the Eye Hospital of Wenzhou Medical University and adhered to the tenets of the Declaration of Helsinki. Written informed consent was obtained from each patient.

Surgical procedure

Two days before surgery, a non-steroidal anti-inflammatory drug (NSAID) drops (Pranopulin; Senju Pharmaceutical, Fukusaki Plant, Japan) was used four times per day for both groups. Before surgery, all patients underwent pupil dilation with compound tropicamide eyedrops (Zhuobian; Xingqi, Shenyang, China) and topical anaesthesia with proparacaine hydrochloride eyedrops (Alcaine; Alcon, Fort Worth, TX, USA). All surgeries were performed by an experienced surgeon (A-Y Y).

For the control group, immediately after a 2.75-mm temporal clear corneal incision, a mean volume of 100 μl of aqueous humour was collected through the incision with a 27-gauge needle attached to an insulin syringe. Aqueous humour was transferred to sterile plastic tubes and stored at −80°C for analysis (Taube et al. 2012). After the injection of viscoelastic agent (Iviz; Bausch & Lomb Freda, Shandong, China) into the anterior chamber, a sideport incision was made with a 15-degree knife. Continuous curvilinear capsulorhexis with a diameter 0.25 mm smaller than the optical body of the intraocular lens (IOL) was performed manually with a forceps. The dissected anterior capsule was pulled out of the eye with the forceps and drenched in formalin–acetic acid for analysis. The lens was removed using a quick-chop technique by a phacoemulsification platform (Stellaris; Bausch & Lomb, Rochester, NY, USA). The IOL was implanted in the capsular bag. The incision was closed by hydration without sutures.

For the trial group, the femtosecond laser platform (LLS-fs 3D; LensAR) was used to generate capsulotomy with a diameter as described above in the control group, and lens fragmentation into 6 segments. The femtosecond laser system has a cornea non-contact liquid interface. For capsulotomy, the line spacing was set at 18 μm and shot spacing at 5 μm, with laser energy set at 8 μJ, whereas for lens fragmentation, the shot spacing was set at a range of 6 μm to 100 μm, and Z-line spacing at a range of 20 μm to 100 μm, with laser energy set at 10 μJ. Then, patients were transferred to phacoemulsification. The waiting interval from the completion of femtosecond laser operation to the beginning of phacoemulsification was approximately 20 min. Besides the capsulotomy and prefragmentation of lens by femtosecond laser, the phacoemulsification procedure for the trial group was almost same as that for the control group. Aqueous humour and lens capsule were collected as described above in the control group.

Morphology of lens capsule

The formalin-fixed anterior lens capsule was gradually dehydrated by alcohol, transparentized by dimethylbenzene and embedded in paraffin, and then cut into sections of 4 μm thickness. They were stained with haematoxylin–eosin (HE), and the cell morphology was assessed by an experienced pathologist (X-Y Q) who was masked to the surgical options. Then, the lens capsule was taken out after dissolution of the paraffin by heat. Dimethylbenzene was used for further removal of the paraffin from the lens capsule. After washing by gradient alcohol and water, the lens capsule was stained with Wright's Giemsa (WG) stain for assessment of edge morphology under light microscope.

Aqueous humour analysis

The proteins in the aqueous humour were extracted by sodium dodecyl sulphate–polyacrylamide gel electrophoresis (SDS–PAGE) (Behera et al. 2009). The protein strip was cut by a blade. After trypsin digestion of the protein strips, the protein was analysed by a mass spectrometer (Ultraflex III TOF/TOF; Bruker Dalton). The specific procedures were described as follows:
(1) Fading: (i) After cutting, each protein strip was placed in a 0.6-ml EP tube, crumbed by the tip head and washed with Milli-Q water twice. Then, water was sucked. (ii) Fade: the protein was faded by 180 μl 50% MeOH/50 mM NH4HCO3 more than twice, 30 min each time, and then washed with 180 μl Milli-Q water for 5 min, with 180 μl 50% ACN for 5 min and with 180 μl 100% ACN for 5 min. (iii) Alkylate: A total of 50 μl 25 mM DTT/100 mM NH4HCO3 was added into the dry colloidal particles. They were incubated at 55°C for 20 min after swelling. Then, DTT was sucked, and 55 mM IAA/100 mM NH4HCO3 was added into the colloidal particles. They were incubated at room temperature for 20 min. (iv) Dehydrate: After IAA was washed off, they were washed with Milli-Q water for 5 min, with 180 μl 50% ACN for 5 min and with 180 μl 50% ACN for 5 min. Finally, they were dried under vacuum for 30 min.
(2) Digestion: (i) The pancreatin was diluted to 20 ng/μl with 25 mM NH4HCO3. A total of 3 μl pancreatin was added into each tube of colloidal particles, and it was bathed with ice for 15 min. The colloidal particles were immersed by about 3 μl 25 mM NH4HCO3 after redundant pancreatin was washed off. (ii) The EP tube was reversed carefully, and the whole shelf was put into the plastic case and kept in water bath at 37°C for 16 hr for digestion. (iii) The plastic case was taken out and cooled to ambient temperature. (iv) A total of 10 μl 25 mM NH4HCO3 was added into the EP tube and shocked for 15 min. The supernatants were collected to the second tube, and 10 μl 2.5% TFA was added. The second tube was shocked for 5 min. The supernatants were collected to the third tube, and 10 μl 2.5% TFA–50% CAN was added. The third tube was shocked for 5 min. The supernatants were collected to the fourth tube, and 10 μl 100% ACN was added. The fourth tube was shocked for 5 min, and the supernatants were collected to a new tube. (v) The drips were concentrated to 5–10 μl under vacuum, and then, 20 μl 0.5% TFA was added and concentrated to 10–20 μl.

(3) Point target: (i) Each drain sample was added into 1.5 μl weight solution (30% CAN contained 0.1% TFA; the rest was filled with water) and shocked for 1 min. Weight solution was absorbed from the bottom of the pipe and the wall was rinsed several times using weight solution to dissolve the peptides on the tube wall; then, the weight solution at the bottom of the pipe was repeatedly blown 6–7 times. (ii) The new spear was put on to absorb 0.8 μl sample. The droplet was squeezed out and hanged from the spear tip and then gently pointed in holes in the steel target (Applied Biosystems, Foster, CA, USA) without being touched the steel target. (iii) The steel target was dried in a clean place. After the drop in the hole dried fully, the rest of the weight solution was pointed to the same hole. The operation was repeated until all the sample solutions were pointed in the holes. (iv) After the last point, when about a third of the droplet evaporated into the original volume, 0.5 μl matrix (5 mg/ml HCCA, 50% ACN containing 0.1% TFA) was added into the sample. Mass spectrometric detection was performed when the sample dried fully.

(4) Mass spectrometry analysis: Signal was collected with settings of UV wavelength 355 nm, repeat rate 200 HZ, acceleration voltage 20 000 V, the best quality resolution 1500 Da and scanning mass range 700–3200 Da. The mass spectrometer was calibrated by the internal standard of the cutting peak of pancreatic enzyme. Mass spectrogram of all experimental samples was obtained using the default mode. The flexAnalysis software (Bruker Dalton) was used to filter baseline peaks and identify signal peaks. The BioTools software (Bruker Dalton) was used to search NCBI database, look for matched protein and query its function to explicit the kind of the identified protein.

(5) Query condition: The query conditions were as follows: (i) Peptide mass range: 800–4000 Da; (ii) Error range of apparent PI and apparent Mr: no limitation; (iii) The level of mass spectrum quality error range: 50 ppm; (iv) The quality of secondary spectrum error range: 0.6 Da; (v) Missed cleavages (missing enzyme loci): one; (vi) Charge: +1; (vii) Monoisotopic; (viii) Global Modification: carbamidomethyl; (ix) Variable modification: oxidation; (x) Variable modification: oxidation; and (xi) Homo sapiens (human).

Electrolyte in the aqueous humour was detected by a chemistry analyzer (Aeroset Clinical Chemistry Analyzer; Abbott Laboratories).

Statistical analysis

All statistical analyses were performed using a commercial software (SPSS 16.0; SPSS, Chicago, IL, USA). Student's *t*-test was used to compare the means of grouped continuous variables. Chi-square test was used to analyse nucleus hardness of cataract. The level of significance was $p < 0.05$.

Results

Thirty-nine eyes were enrolled in this study. The demographics of the patients are shown in Table 1, and there was no significant difference between the two groups. All patients underwent an uneventful surgery. Complications such as miosis, incomplete capsulotomy and capsule rupture did not occur.

Light microscope assessment of the anterior lens capsule revealed tags under magnification of 40× (Fig. 1A) and saw-teeth under magnification of 200× and 400× (Fig. 1C,E) along the edge of the capsulorhexis in the trial group, while the edge was smooth in the control group (Fig. 1B,D,F). Intact cells were found in the area boundary to the cutting edge of the anterior lens capsule under magnification of 200× and 400× in the two groups (Fig. 1C, D,E,F). Haematoxylin-eosin (HE) staining showed intact cells in the region near to the cutting edge of the anterior lens capsule under magnification of 400× in the two groups, and there was no between-groups difference in the cellular morphology (Fig. 1G,H).

The mass spectrometry analysis of proteins in aqueous humour revealed albumin in both groups (Figs 2 and 3), and β-crystallin B1, γ-crystallin S and transferrin in the trial group (Figs 4, 5 and 6).

Table 2 shows the analysis of electrolyte in the aqueous humour. There was a significant difference in the concentrations of K^+, Na^+ and Cl^- between the two groups. The concentrations of Ca^{2+}, Mg^{2+} and P^{3-} did not differ significantly between the two groups.

Discussion

Femtosecond laser-assisted cataract surgery (FLACS) has been shown to have some advantages over conventional phacoemulsification and appears to be a type of new technology to further improve the curative effect of cataract surgery. Femtosecond laser-assisted lens fragmentation significantly reduced phacoemulsification time and energy compared with conventional techniques (Nagy et al. 2009; Palanker et al. 2010; Friedman et al. 2011; Yu et al. 2015). Ultrasound energy may damage surrounding structures and may be implicated in the pathogenesis of endothelial cell loss (Dick et al. 1996). Thus, FLACS causes less damage to corneal endothelial cells and may result in less corneal swelling in the early postoperative period than conventional phacoemulsification (Takács et al. 2012). Femtosecond laser-assisted capsulotomy is more precise, accurate and repeatable than conventional techniques (Friedman et al. 2011; Yu et al. 2015). The improvement in capsulotomy diameter and regularity has been linked with significantly better IOL

Table 1. The demographics of the patients.

	Trial group	Control group	p value
Cases	19 eyes (13 patients)	20 eyes (17 patients)	
Gender (F/M)	6/7	9/8	
Age (Years)	64.2 ± 11.2	71.0 ± 11.7	0.12
Best corrected visual acuity (LogMAR)	0.88 ± 0.67	0.70 ± 0.46	0.36
Nucleus hardness			
II	4	0	
III	8	11	
IV	6	4	
V	1	5	0.06*

* Chi-square test.

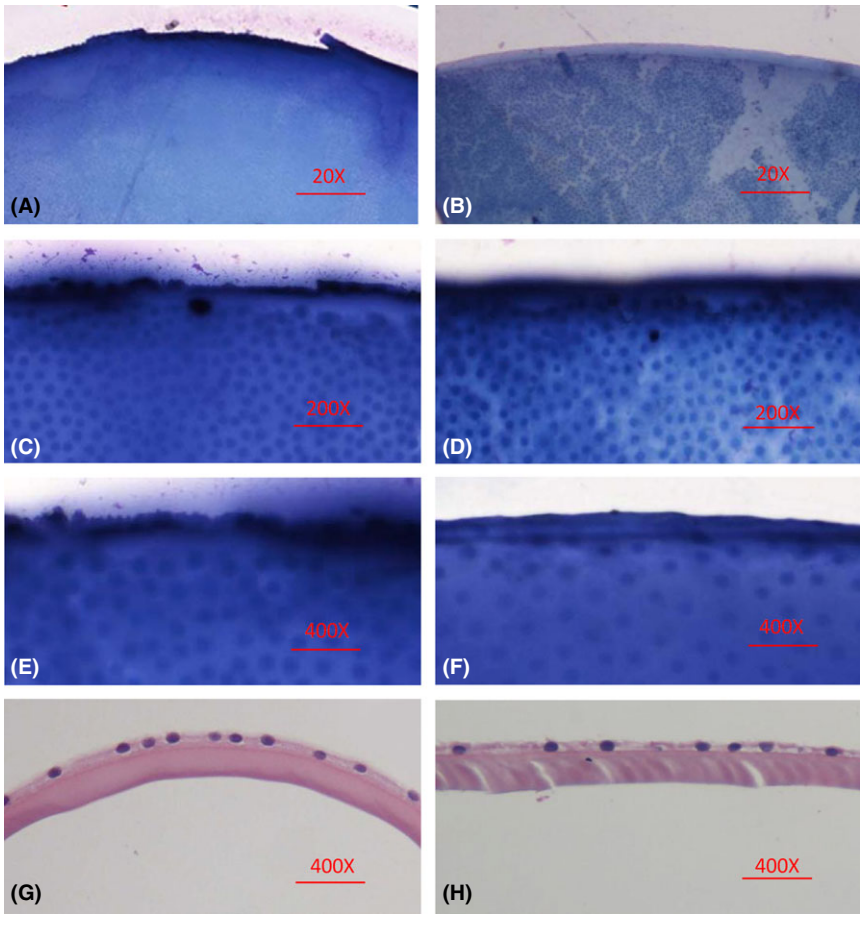

Fig. 1. Morphology of the anterior lens capsule under light microscope. (A) Wright's Giemsa (WG) staining of the cutting edge in the trial group (40×); (B) WG staining of the cutting edge in the control group (40×); (C) WG staining of the cutting edge in the trial group (200×); (D) WG staining of the cutting edge in the control group (200×); (E) WG staining of the cutting edge in the trial group (400×); (F) WG staining of the cutting edge in the control group (400×); (G) Haematoxylin-eosin (HE) staining of the region near to the cutting edge in the trial group (400×); (H) HE staining of the region near to the cutting edge in the control group (400×).

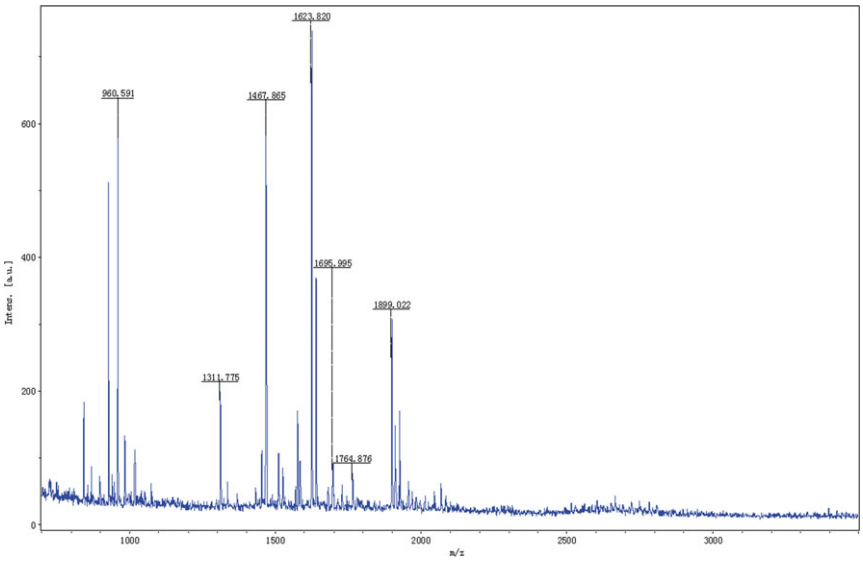

Fig. 2. The mass spectrometry analysis of proteins in aqueous humour in the control group. It showed peptide mass fingerprinting of albumin.

centration (Nagy et al. 2009, 2011; Kránitz et al. 2011, 2012). There is early evidence of more predictable refractive outcomes resulting from improved effective lens position (Filkorn et al. 2012; Yu et al. 2015). What's more, FLACS can be tried in complex cases such as Marfan's syndrome and paediatric cataract (Abouzeid & Ferrini 2014; Crema et al. 2015; Dick et al. 2015). However, FLACS delivers first the capsulotomy and then lens fragmentation by femtosecond laser; thus, the questions are whether toxic substances are produced when femtosecond laser interacts with lens and capsular, and whether such substances are released to aqueous humour from the capsulotomy gap during the waiting time between the completion of the femtosecond laser operation and the beginning of phacoemulsification. These concerns need to be answered as FLACS has been increasingly accepted in clinics.

The femtosecond laser-assisted capsulotomy had different appearance of cutting edge under light microscopy from that by manual capsulorhexis. The cutting edge was tag- and saw-tooth-shaped in the femtosecond laser-assisted capsulotomy (Fig. 1A,C,E) compared with the smooth edge in the control group (Fig. 1B,D,F). This might be explained by the minimal torsional movements of the eye during the release of femtosecond laser (Ostovic et al. 2013; Kohnen et al. 2014). In addition, the femtosecond laser acts in the way of pulse not continuous, and may exist incomplete overlaps of each laser spot. In previous researches of morphological changes in the edge structures after femtosecond laser-assisted capsulotomy, both light microscopy and electron microscopy showed a saw-tooth pattern with individual grooves on the cut edge with increasing magnification (Ostovic et al. 2013; Kohnen et al. 2014). Femtosecond laser-assisted capsulotomy had less average resistance to capsule tear than manual capsulorhexis, and a capsulotomy created at a high laser energy was slightly weaker and less extensible than that created at low or intermediate levels in *ex vivo* porcine possibly due to the increased thermal effect (Sándor et al. 2014, 2015). The respiratory movement of the eye during femtosecond laser-assisted capsulotomy was speculated as a potential risk factor for redial capsule tear (Schultz et al.

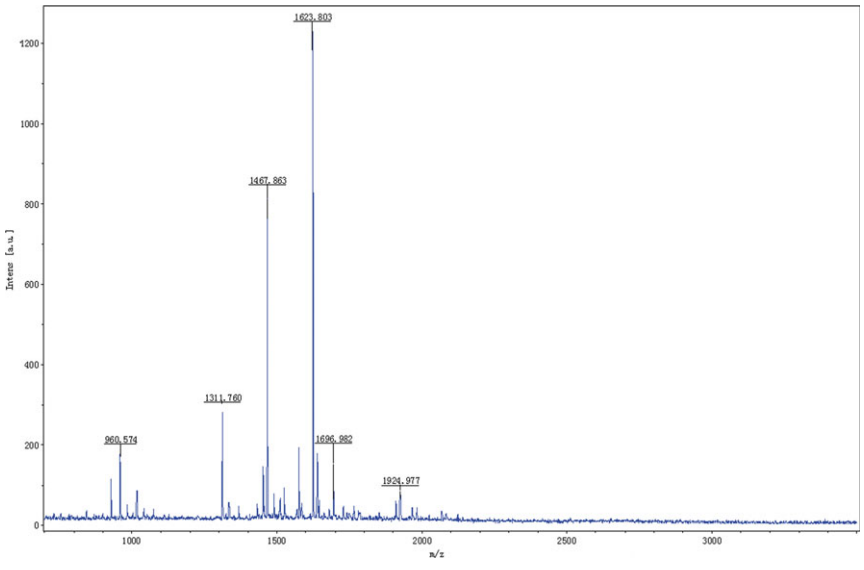

Fig. 3. The mass spectrometry analysis of proteins in aqueous humour in the trial group. It showed peptide mass fingerprinting of albumin.

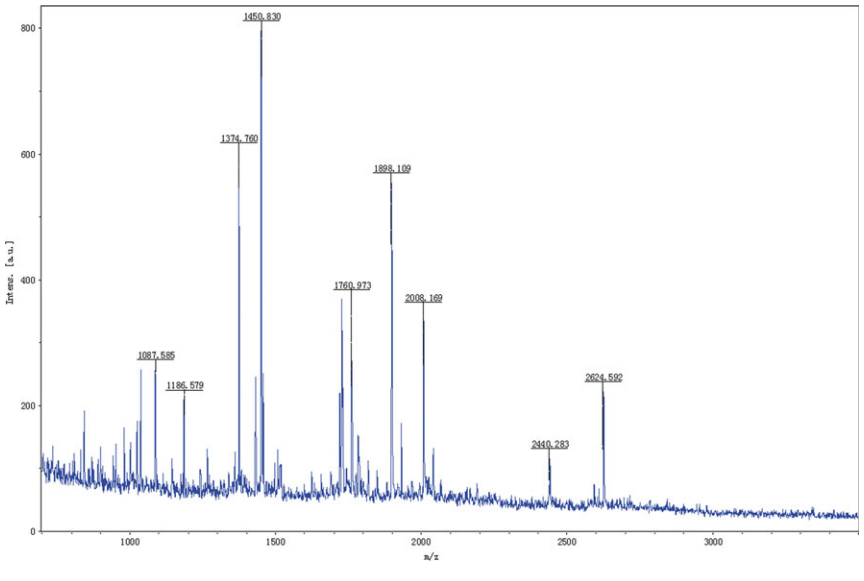

Fig. 4. The mass spectrometry analysis of proteins in aqueous humour in the trial group. It showed peptide mass fingerprinting of β-crystallin B1.

2015a,b). Although the capsular edge in the trial group was saw-toothed under high magnification, it appeared almost smooth as same as manual capsulorhexis under low magnification, and there was no occurrence of incomplete capsulotomy or capsule rupture in this study. The risk of incomplete capsulotomy may include, but not limited to, capsule rupture as surgeons try to pull and take away the capsulotomy. The anterior capsule tear rates ranged from 0% to 1.9% (Conrad-Hengerer et al. 2012, 2013; Abell et al. 2013, 2014; Day et al. 2014; Nagy et al. 2014). The slightest attachment of the capsulotomy to the capsule may cause capsular extension, which may lead to lens nucleus drop. Another potential side-effect is that, due to the incomplete capsulotomy, the centration of IOLs may be off and may reduce the postoperative visual performance. Taking the improved accuracy and repeatability of capsulotomy into account, femtosecond laser-assisted capsulotomy is a feasible approach for cataract surgery.

Light microscopy in this study revealed intact cells along the cutting edge of the anterior lens capsule in both groups (Fig. 1C,D,E,F). Even under the magnification of 400×, the cellular morphology of the region near to the cutting edge in both groups was all intact (Fig. 1G,H). This is different from what reported in the literature, in which they found a cell-free area boundary to the cutting edge and a prominent demarcation line on the anterior lens capsule by femtosecond laser (Lensx; Alcon) at magnifications higher than 20× with light microscopy (Ostovic et al. 2013; Kohnen et al. 2014). Electron microscopy is important to assess the fine microanatomic structures of lens capsule specimens. It was able to show individual laser spots and grooves at magnifications higher than 100×; the individual fibres of the capsule at magnifications higher than 3000×; and frayed tissue-, valley- and mountain-like structures at magnifications higher than 10 000× (Ostovic et al. 2013; Kohnen et al. 2014). This difference in the findings of the cellular morphology of the cutting edge might be explained by the following: (i) The difference in femtosecond laser platform. The femtosecond laser parameters they used are as follows: pulse energy 15 μJ, spot separation 4 μm, layer separation 3 μm with a rigid curved interface (Lensx; Alcon); and the expanding cavitation bubble in combination with the pulse energy of femtosecond laser may destruct the cell boundary to the cutting edge of anterior capsule, resulting in a demarcation on anterior capsule (Ostovic et al. 2013; Kohnen et al. 2014). Mayer et al. (2014) found that cell death reaction depended on the laser pulse energy settings and could be reduced to the level observed in a manual capsulorhexis. (ii) Cellular damage during specimen processing. The upside down of capsule, and friction especially at the edge of capsule during specimen processing may lead to displacement and destruction of cells close to the cutting edge of anterior capsule.

The mass spectrometry analysis of proteins in aqueous humour revealed albumin in both groups. Aqueous humour contains a certain amount of protein, mainly albumin, under normal physiological conditions. However, transferrin, β-crystallin B1 and γ-crystallin S were detected in the aqueous humour in the trial group. The reason for this between-group difference is that aqueous humour in trial group was extracted after capsulotomy and lens fragmentation by femtosecond laser, and transferrin and crystallin

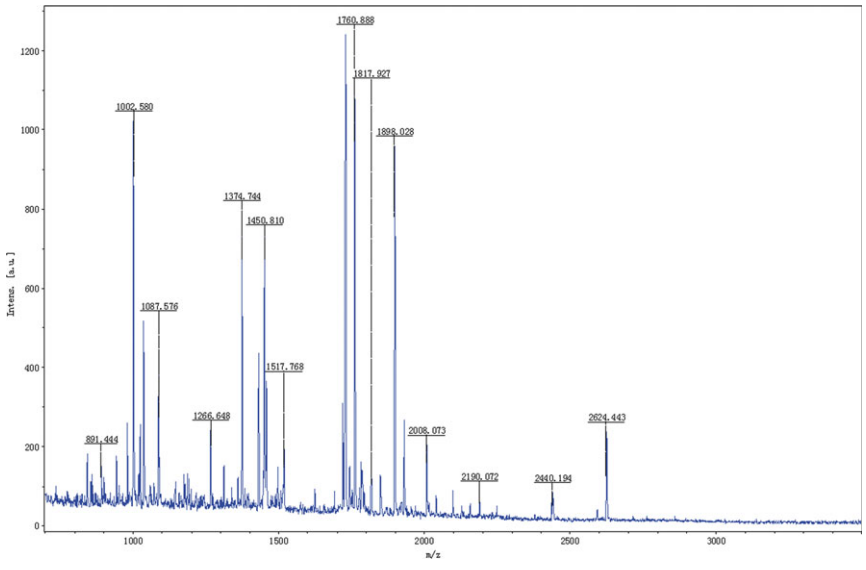

Fig. 5. The mass spectrometry analysis of proteins in aqueous humour in the trial group. It showed peptide mass fingerprinting of γ-crystallin S.

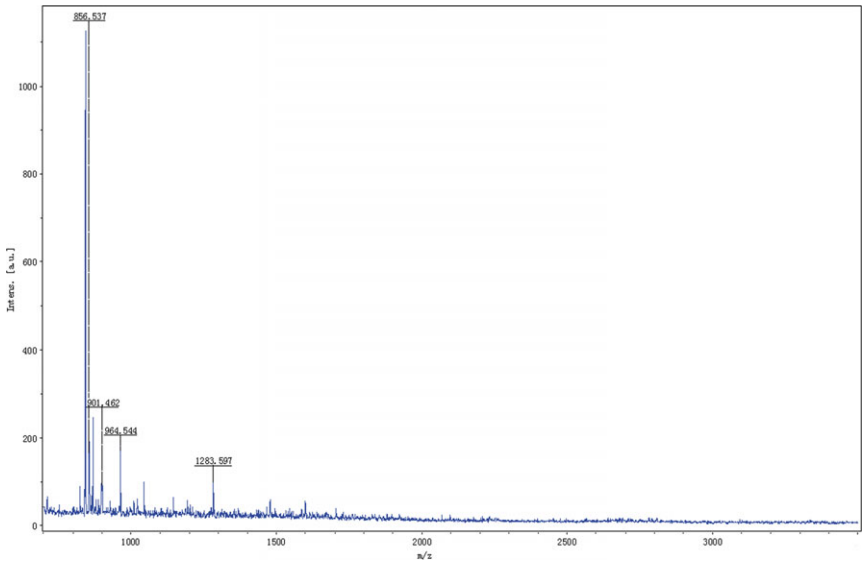

Fig. 6. The mass spectrometry analysis of proteins in aqueous humour in the trial group. It showed peptide mass fingerprinting of transferrin.

Table 2. The analysis of electrolyte in aqueous humour.

	Trial group (mmol/l)	Control group (mmol/l)	p value
K^+	4.75 ± 0.61	4.08 ± 0.21	0.02
Na^+	138.24 ± 10.23	147.83 ± 2.17	0.03
Cl^-	115.69 ± 8.70	123.51 ± 1.93	0.04
Ca^{2+}	1.21 ± 0.10	1.30 ± 0.06	0.10
Mg^{2+}	0.68 ± 0.76	0.68 ± 0.14	0.95
P^{3-}	0.64 ± 0.10	0.60 ± 0.08	0.54

were released to aqueous humour through the capsular gap after femtosecond laser interacted with lens. In contrast, aqueous humour in the control group was extracted before capsulorhexis, so transferrin and crystallin were isolated by the intact capsule and they were not detected from the aqueous humour. Albumin, transferrin and crystallin are all autologous ingredients, and their toxicity to the surrounding ocular tissue had not been reported in the literature, except for the phacoanaphylaxis. There is no significant clinical meaning of the release of transferrin and crystallin from lens to aqueous humour due to FLACS.

The analysis of electrolyte in the aqueous humour revealed a significantly higher concentration of K^+, and lower concentration of Na^+ and Cl^- in the trial group compared to the control group. This might be explained by the communication of these components through the capsular gap after femtosecond laser-assisted capsulotomy and lens fragmentation. In addition, femtosecond laser-assisted capsulotomy and lens fragmentation may affect the ion channels of lens regardless of the unchanged cellular morphology of anterior lens capsule (Fig. 1G). However, the specific mechanism needs further investigations. The electrolyte in the aqueous humour is replaced by the balanced salt solution during the process of phacoemulsification; therefore, the difference in electrolyte concentration has no clinical significance.

No miosis occurred due to FLACS in this study as it may be explained by the following: (i) Few bubble formation due to optimizing the energy setting. Bubble formation from laser energy releases small amounts of free radicals in the anterior chamber, thus triggering pupillary constriction (Nagy et al. 2014). (ii) High automation of the femtosecond laser operation system. During laser programming, the capsulotomy diameter was automatically verified to be smaller than the pupillary diameter due to the system's features of non-contact to cornea, 3-dimensional image reconstruction, automatic pupil centre location and lens position tilting compensation, reducing the possibility of iris trauma (Yu et al. 2015). (iii) Administering a NSAID therapy. Some studies had shown high levels of total prostaglandin and prostaglandin E2 in the aqueous humour during anterior capsulotomy, suggesting their contribution to miosis (Schultz et al. 2013, 2015a,b). Nonsteroidal anti-inflammatory drugs (NSAIDs) are prostaglandin synthesis inhibitors and can reduce prostaglandin concentration in the aqueous humour, which may help to circumvent this reaction and laser-induced miosis (Schultz et al. 2013, 2015a,b).

In conclusion, FLACS causes release of transferrin and crystallin from lens to aqueous humour, and resulted in signif-

icant changes in the concentrations of K^+, Na^+ and Cl^- in aqueous humour. However, these changes due to FLACS have no clinical meaning of toxicity to the surrounding ocular tissue.

References

Abell RG, Kerr NM & Vote BJ (2013): Toward zero effective phacoemulsification time using femtosecond laser pretreatment. Ophthalmology **120**: 942–948.

Abell RG, Davies PE, Phelan D, Goemann K, McPherson ZE & Vote BJ (2014): Anterior capsulotomy integrity after femtosecond laser-assisted cataract surgery. Ophthalmology **121**: 17–24.

Abouzeid H & Ferrini W (2014): Femtosecond-laser assisted cataract surgery: a review. Acta Ophthalmol **92**: 597–603.

Alio JL (2011): Cataract surgery with femtosecond lasers. Saudi J Ophthalmol **25**: 219–223.

Behera B, Das AB & Mohanty P (2009): Changes of soluble proteins in leaf and thylakoid exposed in high saline condition of a mangrove taxa Bruguiera gymnorrhiza. Physiol Mol Biol Plants **15**: 53–59.

Conrad-Hengerer I, Hengerer FH, Schultz T & Dick HB (2012): Effect of femtosecond laser fragmentation of the nucleus with different softening grid sizes on effective phaco time in cataract surgery. J Cataract Refract Surg **38**: 1888–1894.

Conrad-Hengerer I, Al Juburi M, Schultz T, Hengerer FH & Dick HB (2013): Corneal endothelial cell loss and corneal thickness in conventional compared with femtosecond laser–assisted cataract surgery: three-month follow-up. J Cataract Refract Surg **39**: 1307–1313.

Crema AS, Walsh A, Yamane IS, Ventura BV & Santhiago MR (2015): Femtosecond laser-assisted cataract surgery in patients with Marfan syndrome and subluxated lens. J Refract Surg **31**: 338–341.

Day AC, Gartry DS, Maurino V, Allan BD & Stevens JD (2014): Efficacy of anterior capsulotomy creation in femtosecond laser-assisted cataract surgery. J Cataract Refract Surg **40**: 2031–2034.

Dick HB, Kohen T, Jacobi FK & Jacobi KW (1996): Long-term endothelial cell loss following phacoemulsification through a temporal clear corneal incision. J Cataract Refract Surg **22**: 63–71.

Dick HB, Schelenz D & Schultz T (2015): Femtosecond laser-assisted pediatric cataract surgery: Bochum formula. J Cataract Refract Surg **41**: 821–826.

Filkorn T, Kovács I, Takács A, Horváth E, Knorz MC & Nagy ZZ (2012): Comparison of IOL power calculation and refractive outcome after laser refractive cataract surgery with a femtosecond laser versus conventional phacoemulsification. J Refract Surg **28**: 540–544.

Friedman NJ, Palanker DV, Schuele G et al. (2011): Femtosecond laser capsulotomy. J Cataract Refract Surg **37**: 1189–1198.

Hansen A, Geneaux R, Gunther A, Kruger A & Ripken T (2013): Lowered threshold energy for femtosecond laser induced optical breakdown in a water based eye model by aberration correction with adaptive optics. Biomed Opt Express **4**: 852–867.

He L, Sheehy K & Culbertson W (2011): Femtosecond laser-assisted cataract surgery. Curr Opin Ophthalmol **22**: 43–52.

Kohnen T, Klaproth OK, Ostovic M, Hengerer FH & Mayer WJ (2014): Morphological changes in the edge structures following femtosecond laser capsulotomy with varied patient interfaces and different energy settings. Graefes Arch Clin Exp Ophthalmol **252**: 293–298.

Kránitz K, Takacs A, Miháltz K, Kovács I, Knorz MC & Nagy ZZ (2011): Femtosecond laser capsulotomy and manual continuous curvilinear capsulorrhexis parameters and their effects on intraocular lens centration. J Refract Surg **27**: 558–563.

Kránitz K, Miháltz K, Sándor GL, Takacs A, Knorz MC & Nagy ZZ (2012): Intraocular lens tilt and decentration measured by Scheimpflug camera following manual or femtosecond laser-created continuous circular capsulotomy. J Refract Surg **28**: 259–263.

Krarup T, Holm LM, la Cour M & Kjaerbo H (2014): Endothelial cell loss and refractive predictability in femtosecond laser-assisted cataract surgery compared with conventional cataract surgery. Acta Ophthalmol **92**: 617–622.

Mayer WJ, Klaproth OK, Ostovic M, Terfort A, Vavaleskou T, Hengerer FH & Kohnen T (2014): Cell death and ultrastructural morphology of femtosecond laser-assisted anterior capsulotomy. Invest Ophthalmol Vis Sci **55**: 893–898.

Nagy Z, Takacs A, Filkorn T & Sarayba M (2009): Initial clinical evaluation of an intraocular femtosecond laser in cataract surgery. J Refract Surg **25**: 1053–1060.

Nagy ZZ, Kránitz K, Takacs AI, Miháltz K, Kovács I & Knorz MC (2011): Comparison of intraocular lens decentration parameters after femtosecond and manual capsulotomies. J Refract Surg **27**: 564–569.

Nagy ZZ, Takacs AI, Filkorn T et al. (2014): Complications of femtosecond laser-assisted cataract surgery. J Cataract Refract Surg **40**: 20–28.

Ostovic M, Klaproth OK, Hengerer FH, Mayer WJ & Kohnen T (2013): Light microscopy and scanning electron microscopy analysis of rigid curved interface femtosecond laser–assisted and manual anterior capsulotomy. J Cataract Refract Surg **39**: 1587–1592.

Palanker DV, Blumenkranz MS, Andersen D et al. (2010): Femtosecond laser-assisted cataract surgery with integrated optical coherence tomography. Sci Transl Med **2**: 58ra85.

Rossi M, Di Censo F, Di Censo M & Oum MA (2015): Changes in aqueous humor pH after femtosecond laser-assisted cataract surgery. J Refract Surg **31**: 462–465.

Sándor GL, Kiss Z, Bocskai ZI et al. (2014): Comparison of the mechanical properties of the anterior lens capsule following manual capsulorhexis and femtosecond laser capsulotomy. J Refract Surg **30**: 660–664.

Sándor GL, Kiss Z, Bocskai ZI et al. (2015): Evaluation of the mechanical properties of the anterior lens capsule following femtosecond laser capsulotomy at different pulse energy settings. J Refract Surg **31**: 153–157.

Schultz T, Joachim SC, Kuehn M & Dick HB (2013): Changes in prostaglandin levels in patients undergoing femtosecond laser-assisted cataract surgery. J Refract Surg **29**: 742–747.

Schultz T, Joachim SC, Stellbogen M & Dick HB (2015a): Prostaglandin release during femtosecond laser-assisted cataract surgery: main inducer. J Refract Surg **31**: 78–81.

Schultz T, Joachim SC, Tischoff I & Dick HB (2015b): Histologic evaluation of in vivo femtosecond laser-generated capsulotomies reveals a potential cause for radial capsular tears. Eur J Ophthalmol **25**: 112–118.

Takács AI, Kovács I, Miháltz K, Filkorn T, Knorz MC & Nagy ZZ (2012): Central corneal volume and endothelial cell count following femtosecond laser-assisted refractive cataract surgery compared to conventional phacoemulsification. J Refract Surg **28**: 387–391.

Taube AB, Hardenborg E, Wetterhall M, Artemenko K, Hanrieder J, Andersson M, Alm A & Bergquist J (2012): Proteins in aqueous humor from cataract patients with and without pseudoexfoliation syndrome. Eur J Mass Spectrom **18**: 531–541.

Yu AY, Ni LY, Wang QM, Huang F, Zhu SQ, Zheng LY & Su YF (2015): Preliminary clinical investigation of cataract surgery with a non-contact femtosecond laser system. Lasers Surg Med **47**: 698–703.

Received on August 20th, 2015.
Accepted on January 22nd, 2016.

Correspondence:
A-Yong Yu
270 Xueyuan West Road
Wenzhou
325000 Zhejiang
China
Tel: +86-577-88068880
Fax: +86-577-88830832
Email: yaybetter@hotmail.com

Clinical trial registration: NCT02492659, https://register.clinicaltrials.gov

This work was funded by the Zhejiang Provincial Natural Science Foundation of China (Grant No. Y2110784), Zhejiang Provincial Foundation of China for Distinguished Young Talents in Medicine and Health (Grant No. 2010QNA018), and International Cooperation Project of the Science and Technology Bureau of Zhejiang province, China (Grant No. 2013C14010).

A-Y Y and Q-M W designed the study and reviewed the manuscript; C-X L, M-Q Z and X-Y Q conducted the study; A-Y Y, C-X L, M-Q Z and X-Y Q analysed and interpreted the data; and A-Y Y and C-X L prepared the manuscript.

The research protocol adhered to the tenets of the Helsinki Declaration and was approved by the local ethics committee (Ethics Committee at the Eye Hospital, Wenzhou Medical University, 270 Xueyuan West Road, Wenzhou, Zhejiang, P.R. China). All patients were fully informed about the details and possible risks inherent to this study. Written informed consent was obtained from all patients.